

Technical Notes

Chugging Instability of H_2O_2 Monopropellant Thrusters with Catalyst Reactivity and Support Sizes

Sungkwon Jo* and Dongwuk Jang†

*Korea Advanced Institute of Science and Technology,
Daejeon 305-701, Republic of Korea*

Sungyong An‡

*Korea Institute of Nuclear Safety,
Daejeon 305-338, Republic of Korea*
and

Sejin Kwon§

*Korea Advanced Institute of Science and Technology,
Daejeon, 305-701, Republic of Korea*

DOI: 10.2514/1.B34222

Nomenclature

D	= diameter of reactor, mm
G	= mass flux, g/s/cm^2
L	= length of reactor, mm
\dot{m}	= propellant mass flow rate, g/s
P_c	= reaction-chamber pressure, bar
P_f	= feeding pressure, bar
P_i	= downstream pressure of injector face, bar
T_c	= reaction-chamber temperature, $^\circ\text{C}$
T_i	= downstream temperature of injector face, $^\circ\text{C}$
ΔP_{cat}	= pressure drop across a catalyst bed, bar
ΔP_{inj}	= pressure drop across an injector, bar
η_{C^*}	= efficiency of characteristics velocity, %

I. Introduction

HIGH-PERFORMING storable propellants such as hydrazine (N_2H_4) (a monopropellant) and nitrogen tetroxide (an oxidizer) in bipropellant systems are currently used despite their toxicity. As a result of the growing concerns and regulations related to the environment, interest in rocket-grade hydrogen peroxide (one of the oldest propellants) as an alternative propellant has grown since the mid-1990s because of its nontoxic, storable characteristics [1,2].

When hydrogen peroxide is used as a propellant, almost all propulsion systems need a catalyst bed to decompose it into oxygen and steam, generating high pressure and temperature. Catalyst and catalyst-bed design are of great importance in monopropellant

thrusters, as well as gas generators and bipropellant propulsion systems, because they affect the decomposition capacity, pressure instability, and response time. Some studies have investigated the catalyst in terms of catalyst reactivity and catalytic support effect [3–11]. For applications of hydrogen peroxide in monopropellant thrusters, a wide variety of methodologies to determine catalyst-bed size, the effects of injector type and ullage volume, decomposition efficiency, and response time in various-scale thrusters have been examined and reported [12–18]. Although many studies have been carried out on the action of various catalysts to decompose hydrogen peroxide and on the performance of hydrogen peroxide propulsion systems, there are few experimental results regarding pressure instability with respect to catalyst reactivity and support size in monopropellant thrusters.

Recently, a study regarding chugging instability with a MnO_2 catalyst in monopropellant thrusters was reported [18]. Another investigation was carried out to understand the effect of catalyst reactivity and support size in three monopropellant thrusters with different aspect ratios (L/D). In the present study, a MnO_2 -mixed PbO catalyst coated with two different catalytic support sizes (10–16 mesh and 16–20 mesh) was evaluated under different operating pressure conditions.

II. Test Apparatus

A. Propellant, Catalyst, and Catalytic Support

In the present study, hydrogen peroxide with a concentration of 90 wt% (Peroxide Propulsion, Sweden) was used in all experiments. The quality of hydrogen peroxide was in accordance with the requirements of MIL-PRF-16005F [19], which defines the maximum allowable impurities for rocket-grade hydrogen peroxide. The propellant density was 1392 kg/m^3 at 20°C and the theoretical adiabatic temperature and characteristic velocity at nominal chamber pressure of 20 bar [as calculated by the Chemical Equilibrium and Applications (CEA) program [20]] were 749°C and 936.4 m/s , respectively.

MnO_2 was used broadly as a catalyst for hydrogen peroxide decomposition. In addition to the MnO_2 , several materials as additives have been studied to enhance decomposition reactivity. Prior studies have reported that the activity of MnO_2 increased when promoters such as Zn, Ni, Cu, Bi, Ce, and Pb were added [4–6]. In this study, Pb was selected as an additive material to enhance the reactivity of MnO_2 [6]. Bimodal-type Al_2O_3 (Alfa Aesar) was used as a catalytic support; it has a surface-area-to-mass ratio of approximately $255 \text{ m}^2/\text{g}$. Granules with mesh sizes of 10–16 (1.18–2.0 mm) and 16–20 (0.85–1.18 mm) were prepared from the 1/8 in. Al_2O_3 pellets. Both NaMnO_4 and $\text{Pb}(\text{NO}_3)_2$ (Aldrich) were used as precursors for MnO_2 and PbO , respectively; they were mixed so that the molar weights of Mn (63.2 wt% of MnO_2) and Pb (92.8 wt% of PbO) were identical. The catalyst prepared by impregnating two different sizes of Al_2O_3 granules with the solution of mixed precursors. Impregnation was followed by drying (95°C for 12 h), calcination (500°C for 4 h), and drying (95°C for 12 h) again. After calcination, the catalyst was washed with water to remove Na^+ ions and impurities.

After the coating procedure, the catalyst as shown in Fig. 1 was analyzed by Brunauer–Emmett–Teller (BET), accelerated surface area and porosimetry system (ASAP 2020), and energy dispersive spectroscopy (EDS) methods to confirm surface-area-to-mass ratio, pore volume, average pore size, and coated materials. The elements of Mn and Pb were detected on the surface of the fabricated catalyst by EDS analysis. All measured data are summarized in Tables 1 and 2. From the results of catalyst analysis, Na, as an impurity, was detected to the extent of below 1.0 wt%. The Mn/Pb molar ratios for

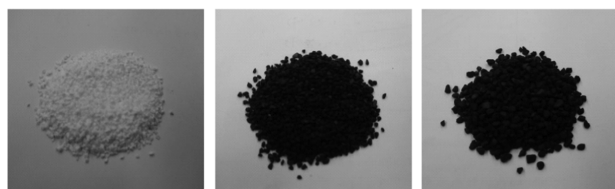
Received 29 December 2010; revision received 25 March 2011; accepted for publication 10 April 2011. Copyright © 2011 by the American Institute of Aeronautics and Astronautics, Inc. All rights reserved. Copies of this paper may be made for personal or internal use, on condition that the copier pay the \$10.00 per-copy fee to the Copyright Clearance Center, Inc., 222 Rosewood Drive, Danvers, MA 01923; include the code 0748-4658/11 and \$10.00 in correspondence with the CCC.

*Ph.D. Candidate, Division of Aerospace, 335 Gwahak-ro, Yuseong-gu; earthcsk@kaist.ac.kr. Member AIAA.

†Graduate Student, Division of Aerospace, 335 Gwahak-ro, Yuseong-gu; menat87@kaist.ac.kr.

‡Senior Researcher, 34 Gwahak-ro, Yuseong-gu; k975asy@kims.re.kr.

§Professor, Division of Aerospace, 335 Gwahak-ro, Yuseong-gu; trumpet@kaist.ac.kr. Member AIAA.



16-20 mesh Al_2O_3 MnO_2+PbO (16-20) MnO_2+PbO (10-16)

Fig. 1 Al_2O_3 catalytic support and catalysts fabricated with different support sizes.

10–16 and 16–20 mesh sizes were 1.06 and 1.12, respectively; these values indicate slightly excess manganese. This result may have been caused by the differences in the adhesion characteristics of the Al_2O_3 surface and the catalyst particle size.

B. Monopropellant Thrusters

In the previous study, the MnO_2 catalyst was examined with different catalytic reactor aspect ratios [18]. Monopropellant thrusters with three different aspect ratios were designed to be nearly identical to those of the prior study to enable easy comparison of the results. Three 50-N-class monopropellant thrusters were prepared with different aspect ratios (0.51, 1.0, and 1.95), but nearly identical volumes ($12.25 \pm 0.02 \text{ cm}^3$). A shower-head-type injector with 15 orifices (orifice diameter of 0.4 mm) was used in all thrusters to supply hydrogen peroxide to the catalytic reactor. The designed thrusters and pressure measurement positions are shown in Fig. 2.

C. Data Acquisition

Hydrogen peroxide was pressurized with regulated nitrogen gas and controlled by a pneumatic actuator operated using a solenoid valve. A Coriolis-type mass flow meter with $\pm 0.5\%$ precision was introduced to measure the propellant flow rate. Five pressure transducers of three different types (35 bar max $\pm 0.12\%$ accuracy, 50 bar max $\pm 0.04\%$ accuracy, and 70 bar max $\pm 0.15\%$ accuracy), a data acquisition card, and signal conditioning extension for instrumentation (SCXI) modules from National Instruments were used to measure the pressure. All tests were performed in pulse mode with a 1.0 s valve-on time and a 1.0 s valve-off time with a sampling rate of 1000 samples/s with a 10 kHz filter.

III. Result and Discussion

The pulse mode tests were performed for each condition. The pressures at each position were measured to determine pressure

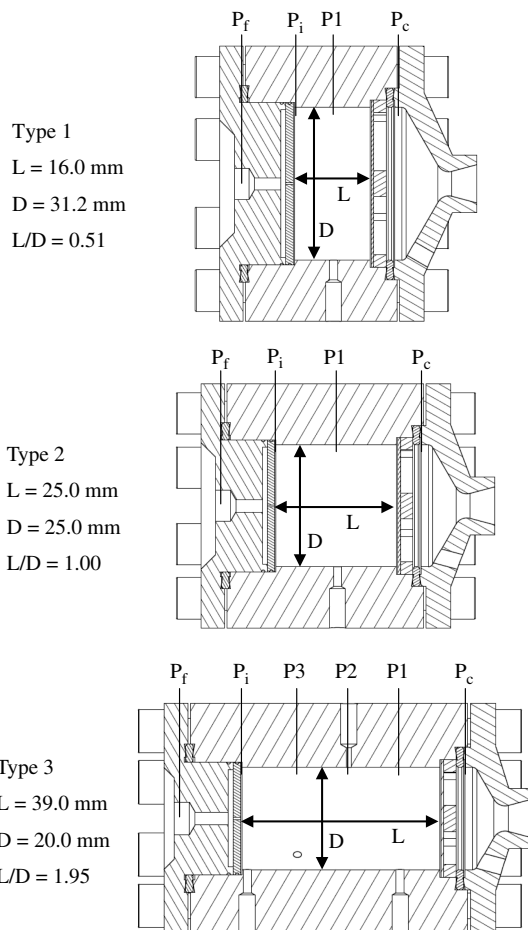


Fig. 2 Test thrusters with different aspect ratios and pressure measurement positions.

variations along the axis direction of the thrusters as well as the pressure drop across the injector ($\Delta P_{\text{inj}}, P_f - P_i$), pressure drop across the catalytic bed ($\Delta P_{\text{cat}}, P_i - P_c$), and instability inside the reaction chamber. All measured mean pressures, mass flow rates, mass fluxes, and characteristic velocity efficiencies are summarized in Table 3.

The low frequency (10–400 Hz) instability, called chugging, mainly appeared in thrusters designed to have low chamber pressures (100–500 psia) [21]. In a study on monopropellant thrusters using a MnO_2 catalyst [18], chugging instability above $\pm 5\%$ was observed, which suggested that a high chamber pressure and low aspect ratio are preferable for reducing the instability in a reaction chamber. To deepen our understanding of chugging instability and to investigate the effect of catalyst reactivity, reaction tests with MnO_2 -mixed PbO catalyst were performed under almost identical conditions to those of the prior study. A chugging instability above $\pm 5\%$ in the reaction chamber, however, could not be observed, indicating a maximum chugging amplitude of $\pm 2.1\%$ in the case of enhanced reactivity compared with a MnO_2 catalyst. In a previous study [18], chugging frequencies reported to be in several tens of hertz; however, a definite peak frequency of chugging instability was not found from the fast Fourier transform results, which showed a nearly constant magnitude at various frequencies. Moreover, the pressures in the high-aspect-ratio thruster (type 3) were considerably stable, unlike those for the MnO_2 catalyst. Although the chugging amplitude tended to increase with decreasing reaction-chamber pressure, a high pressure drop across the catalytic bed, that is, a high aspect ratio, did not appear to affect the chugging instability in the case of the MnO_2 -mixed PbO catalyst.

Two different sizes of catalytic supports were evaluated to compare the pressures along the axis direction of the thrusters and the

Table 1 BET and pore analysis summary of Al_2O_3 and $\text{MnO}_2 + \text{PbO}$ catalyst with two different support sizes

Analysis	Al_2O_3	$\text{MnO}_2 + \text{PbO}/\text{Al}_2\text{O}_3$	
		10–16 mesh	16–20 mesh
BET area, m^2/g	250.3	146.6	160.9
Pore volume, cm^3/g	0.8	0.45	0.45
Average pore size, nm	12.13	12.34	11.3

Table 2 EDS analysis of Al_2O_3 and $\text{MnO}_2 + \text{PbO}$ catalyst with two different support sizes

Element	Al_2O_3	$\text{MnO}_2 + \text{PbO}/\text{Al}_2\text{O}_3$	
		10–16 mesh	16–20 mesh
O, wt%	40.64	26.30	30.73
Al, wt%	59.36	33.07	36.22
Mn, wt%	—	8.76	7.43
Pb, wt%	—	31.10	25.11
Na, wt%	—	0.77	0.51

Table 3 Pressure oscillations of each position and performance in each reaction test

Case	P_c , bar	P_1 , bar	P_2 , bar	P_3 , bar	P_i , bar	P_f , bar	ΔP_{inj} , bar	ΔP_{cat} , bar	\dot{m} , g/s	G , g/(s · cm ²)	η_{c^*} , %	Chugging amplitude ^a , %
<i>Case of 10–16 mesh (average diameter of 1.18–2.0 mm)</i>												
Type 1 (0.51)												
L1-1	7.7	7.8	—	—	7.8	9.1	1.3	0.1	25.6	3.35	54.8	±0.8%
L1-2	16.0	16.2	—	—	16.2	19.4	3.3	0.2	37.8	4.94	76.9	±0.5%
L1-3	23.3	23.7	—	—	23.7	29.5	5.8	0.4	53.8	7.03	78.9	±0.5%
L1-4	No test											
Type 2 (1.00)												
L2-1	7.5	8.8	—	—	8.8	9.4	0.6	1.3	17.7	3.60	76.3	±1.3%
L2-2	14.7	17.6	—	—	17.4	19.7	2.3	2.7	30.6	6.17	86.6	±0.8%
L2-3	21.3	25.8	—	—	25.8	29.9	4.1	4.5	44.2	9.01	87.1	±0.8%
L2-4	27.5	33.6	—	—	33.7	40.2	6.5	6.1	54.5	11.17	91.2	±0.9%
Type 3 (1.95)												
L3-1	6.8	7.9	8.8	8.9	9.0	9.5	0.6	2.1	14.7	4.69	81.7	±1.7%
L3-2	13.6	15.7	17.6	17.8	18.2	20.1	1.9	4.6	24.8	7.88	96.6	±0.9%
L3-3	19.6	22.9	25.7	26.6	26.9	30.1	3.4	7.3	35.3	11.23	97.9	±0.9%
L3-4	25.5	29.9	34.0	34.9	35.2	40.5	5.2	9.8	48.3	15.36	92.9	±0.9%
<i>Case of 16–20 mesh (average diameter of 0.85–1.18 mm)</i>												
Type 1 (0.51)												
S1-1	8.9	9.2	—	—	9.2	10.0	0.8	0.4	21.7	2.84	74.5	±0.7%
S1-2	16.8	17.5	—	—	17.6	19.8	2.2	0.8	35.3	4.62	86.6	±0.4%
S1-3	24.1	25.1	—	—	25.4	29.7	4.3	1.3	55.2	7.22	79.6	±0.4%
S1-4	No test											
Type 2 (1.00)												
S2-1	7.9	9.0	—	—	9.1	10.0	0.8	1.2	17.5	3.57	81.5	±1.4%
S2-2	14.7	17.0	—	—	17.5	19.7	2.2	2.8	30.3	6.17	87.9	±0.7%
S2-3	21.4	25.0	—	—	26.0	30.1	4.1	4.6	44.2	9.01	87.4	±0.6%
S2-4	27.2	32.3	—	—	33.9	40.1	6.3	6.6	54.8	11.17	89.7	±0.5%
Type 3 (1.95)												
S3-1	5.7	7.0	8.4	9.1	9.3	10.0	0.7	3.7	13.3	4.25	74.9	±2.1%
S3-2	11.2	14.2	17.1	18.9	19.5	20.8	1.3	8.3	21.5	6.84	91.4	±0.7%
S3-3	16.1	21.0	25.2	28.3	28.7	31.2	2.5	12.6	30.9	9.82	91.5	±0.7%
S3-4	20.0	27.5	33.1	36.9	37.5	41.1	3.6	17.5	38.2	12.17	92.1	±0.6%

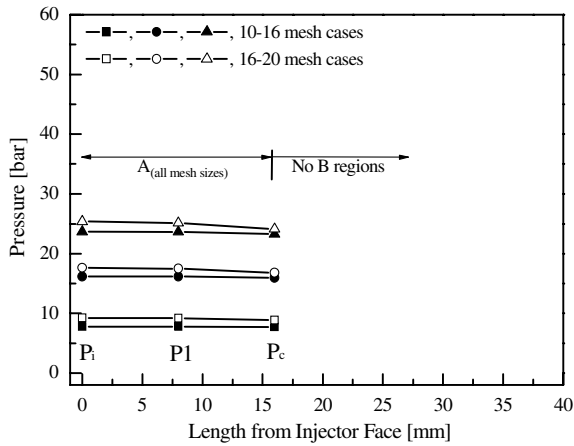
^aCalculated by chamber pressure P_c .

difference of the pressure drop across the catalytic bed. The pressure distributions of the type-3 thruster are shown in Fig. 3. Because the maximum error was approximately ± 0.1 bar from the accuracy of used pressure transducers, the error bars of all test results were small enough to enable the difference between the two mesh sizes to be distinguished. The pressures rarely decreased up to certain lengths from the injector surface and the length was increased with increasing catalytic support size. It seems that the propellant injected by a shower-head-type injector penetrates a certain length of a catalytic bed owing to its high momentum, and decomposes thereafter. In other words, there are two regions of penetration and decomposition. A differential pressure of 1 bar between each measurement position was assumed to divide the penetration (A) and decomposition (B) regions at the highest feed pressure condition in Fig. 3. With increasing aspect ratio, the classification of the two regions grew much clearer. For the type-1 thruster, most characteristic velocity efficiencies were below 80% and displayed a white plume behind the nozzle during the tests, because most of the catalytic bed acted as a region of penetration not decomposition. Figure 4 compares the reaction-chamber temperatures for the L1-1 and L2-2 cases with pressure variation. The L1-1 case, which almost has a penetration region, has a lower chamber temperature profile compared with the L2-2 case. Moreover, the temperature of the reaction chamber increased slowly even though chamber pressure was stable. This slow increase in the low aspect ratio case can be attributed to the fact that a considerable amount of the fed hydrogen peroxide passes through the catalytic bed without decomposition. Neither of the catalytic support sizes could be tested under a feeding pressure above 30 bar to avoid a dangerous situation, because most of the fed propellant was exhausted in liquid phase without decomposition. Therefore, other types of injectors that can enhance the atomization of propellant would be preferable to reduce the penetration region and catalytic bed of H_2O_2 monopropellant thrusters.

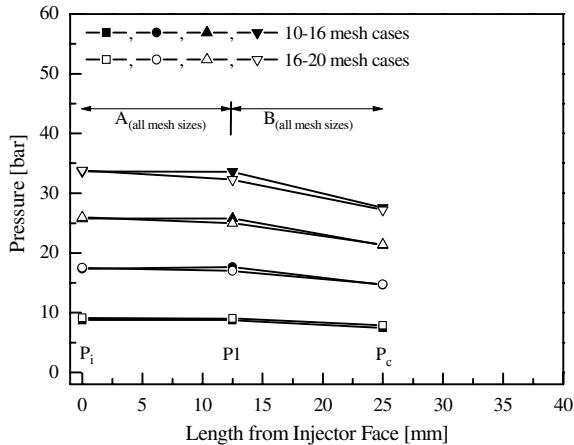
The pressure drop per unit length across the catalytic bed exhibited a linear characteristic with mass flux, as shown in Fig. 5. The pressure drops of 16–20 mesh size was almost doubled compared with the pressure drops of 10–16 mesh size. For the results of the same 16–20 mesh size, pressure drops per unit length were increased with increasing mass flux and aspect ratio. If the pressure drops evenly throughout the reaction chamber, the results for each aspect ratio converge under an identical mass flux. However, the slope of the pressure drops increased when the aspect ratio was varied, because the main pressure drop occurs only in the decomposition region. The result of the type-3 thruster was compared with the result of An et al. [18], as shown in Fig. 5. The slope of the pressure drop exhibited a nearly identical tendency. The pressure drop for the MnO_2 case, however, was much higher than that in the present work, indicating chugging instability. The reason for the increased pressure drop in the prior study could not be determined, but it is likely to be a result of pressure fluctuation inside the reaction chamber.

IV. Conclusions

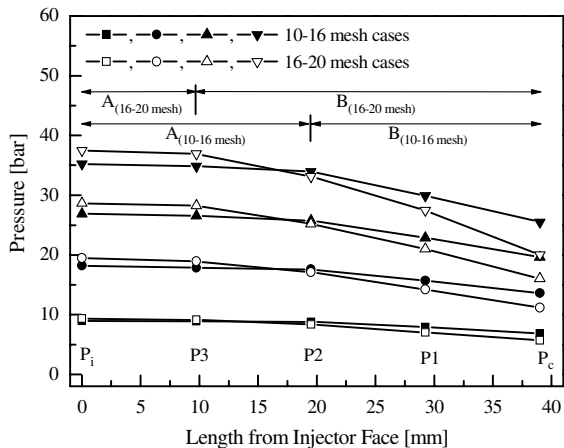
H_2O_2 monopropellant thrusters with three different catalytic bed aspect ratios were tested with a MnO_2 -mixed PbO catalyst to investigate the effect of reactivity and catalytic support size on chugging instability and pressure drop across the catalytic bed. Unlike the previous result of the MnO_2 catalyst, no chugging instability in the reaction chamber was observed by enhancing the catalyst reactivity and all of the pressure variations were quite stable with an oscillation below $\pm 2.1\%$. In other words, the chugging instability in H_2O_2 monopropellant thrusters using a MnO_2 -mixed PbO catalyst are independent with aspect ratios of less than 2.0. The measurement results of pressure distribution along the thrusters suggest that an injector that can atomize well would be preferable to reduce the penetration region and catalytic bed size. Considering the pressure drop across a catalytic bed, a bigger catalytic support size



a) Type 1 thruster



b) Type 2 thruster



c) Type 3 thruster

Fig. 3 Pressure distribution along the axis direction (A: penetration region, B: decomposition region).

would be desirable to reduce the pressure drop under the condition that the catalyst can sufficiently decompose the fed hydrogen peroxide.

Acknowledgment

This work was supported by the Korea Science and Engineering Foundation (KOSEF) grant funded by the Korean Government

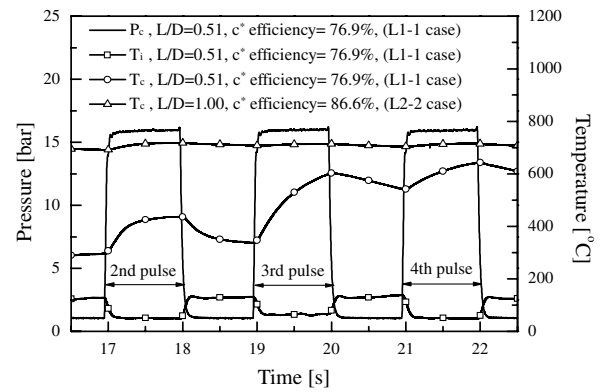


Fig. 4 Pressure and temperature profiles of low-performance case (L1-1) and comparison with stable reaction-chamber temperature case (L2-2).

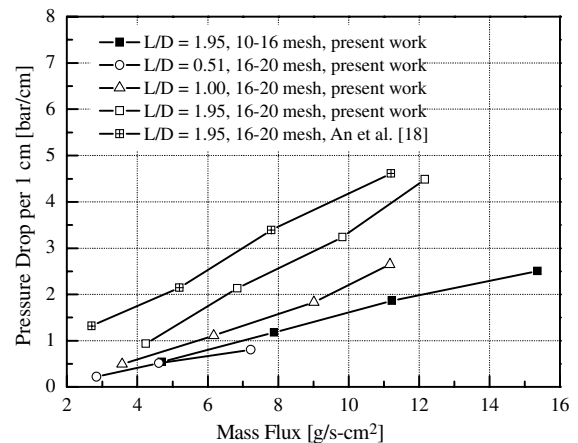


Fig. 5 Pressure drop across catalytic bed (ΔP_{cat}) with respect to mass flux.

(Ministry of Education, Science and Technology) through the National Research Laboratory (no. R0A-2007-000-20065-0).

References

- [1] Ventura, M., and Garboden, G., "A Brief History of Concentrated Hydrogen Peroxide Uses," 35th AIAA/ASME/SAE/ASEE Joint Propulsion Conference & Exhibit, AIAA Paper 1999-2739, Aliso Viejo, CA, June 1999.
- [2] Ventura, M., and Mullens, P., "The Use of Hydrogen Peroxide for Propulsion and Power," 35th AIAA/ASME/SAE/ASEE Joint Propulsion Conference & Exhibit, AIAA Paper 1999-2880, Aliso Viejo, CA, June 1999.
- [3] Rusek, John J., "New Decomposition Catalysts and Characterization Techniques for Rocket-Grade Hydrogen Peroxide," *Journal of Propulsion and Power*, Vol. 12, No. 3, 1996, pp. 574-579. doi:10.2514/3.24071
- [4] El-Aiashy, M. K., Mazhar, H. S., and Kamal, S. M., "Solid-Solid Interaction Between Manganese Carbonate and Zinc Carbonate and the Decomposition of H_2O_2 over Mixed Zinc-Manganese Oxide Catalysts," *Materials Letters*, Vol. 24, 1995, pp. 97-101. doi:10.1016/S0167-577X(95)00070-4
- [5] Hasan, M. A., Zaki, M. I., Pasupulety, L., and Kumari, K., "Promotion of the Hydrogen Peroxide Decomposition Activity of Manganese Oxide Catalysts," *Applied Catalysis A*, Vol. 181, 1999, pp. 171-179. doi:10.1016/S0926-860X(98)00430-X
- [6] Tian, H., Zhang, T., Sun, X., Liang, D., and Lin, L., "A Novel Mixed Metal Oxide Catalyst for the Decomposition of Hydrogen Peroxide," *2nd International Hydrogen Peroxide Propulsion Conference*, Purdue Univ., West Lafayette, IN, Nov. 1999, pp. 199-208.
- [7] Tian, H., Zhang, T., Sun, X., Liang, D., and Lin, L., "Performance and Deactivation of $Ir/\gamma-Al_2O_3$ Catalyst in the Hydrogen Peroxide Monopropellant Thruster," *Applied Catalysis A*, Vol. 210, 2001,

- pp. 55–62.
doi:10.1016/S0926-860X(00)00829-2
- [8] Pirault-Roy, L., Kappenstein, C., Guerin, M., and Eloirdi, R., “Hydrogen Peroxide Decomposition of Various Supported Catalysts Effect of Stabilizers,” *Journal of Propulsion and Power*, Vol. 18, No. 6, 2002, pp. 1235–1241.
doi:10.2514/2.6058
- [9] Kappenstein, C., Pirault-Roy, L., Guerin, M., Wahdan, T., Ali, A. A., Al-Sagheer, F. A., and Zaki, M. I., “Monopropellant Decomposition Catalysts. V. Thermal Decomposition and Reduction of Permanganates as Models for the Preparation of Supported MnOx Catalysts,” *Applied Catalysis A*, Vol. 234, 2002, pp. 145–153.
doi:10.1016/S0926-860X(02)00220-X
- [10] Sorge, A. R., Turco, M., Pilone, G., and Bagnasco, G., “Decomposition of Hydrogen Peroxide on MnO₂/TiO₂ Catalysts,” *Journal of Propulsion and Power*, Vol. 20, No. 6, 2004, pp. 1069–1075.
doi:10.2514/1.2490
- [11] Torre, L., Pasini, A., Romeo, L., Cervone, A., and D’Agostino, L., “Performance of a Monopropellant Thruster Prototype Using Advanced Hydrogen Peroxide Catalytic Beds,” *Journal of Propulsion and Power*, Vol. 25, No. 6, 2009, pp. 1291–1299.
doi:10.2514/1.44354
- [12] An, S., and Kwon, S., “Comparison of Catalyst Support between Monolith and Pellet in Hydrogen Peroxide Thrusters,” *Journal of Propulsion and Power*, Vol. 26, No. 3, 2010, pp. 439–445.
doi:10.2514/1.46075
- [13] Pasini, A., Torre, L., Romeo, L., Cervone, A., and d’Agostino, L., “Testing and Characterization of a Hydrogen Peroxide Monopropellant Thruster,” *Journal of Propulsion and Power*, Vol. 24, No. 3, 2008, pp. 507–515.
doi:10.2514/1.33121
- [14] An, S., and Kwon, S., “Scaling and Evaluation of Pt/Al₂O₃ Catalytic Reactor for Hydrogen Peroxide Monopropellant Thruster,” *Journal of Propulsion and Power*, Vol. 25, No. 5, 2009, pp. 1041–1045.
doi:10.2514/1.40822
- [15] An, S., Brahmi, R., Kappenstein, C., and Kwon, S., “Transient Behavior of H₂O₂ Thruster: Effect of Injector Type and Ullage Volume,” *Journal of Propulsion and Power*, Vol. 25, No. 6, 2009, pp. 1357–1360.
doi:10.2514/1.46731
- [16] Lee, S. L., and Lee, C. W., “Performance Characteristics of Silver Catalyst Bed for Hydrogen Peroxide,” *Aerospace Science and Technology*, Vol. 13, 2009, pp. 12–17.
doi:10.1016/j.ast.2008.02.007
- [17] An, S., Lim, H., and Kwon, S., “Hydrogen Peroxide Thruster Module for Microsatellites with Platinum Supported by Alumina as Catalyst,” 43rd AIAA/ASME/SAE/ASEE Joint Propulsion Conference & Exhibit, AIAA Paper 2007-5467, Cincinnati, OH, 2007.
- [18] An, S., Jin, J., Lee, J., Jo, S., Park, D., and Kwon, S., “Chugging Instability of H₂O₂ Monopropellant Thrusters with Reactor Aspect Ratio and Pressure,” *Journal of Propulsion and Power*, Vol. 27, No. 2, 2011, pp. 422–427.
doi:10.2514/1.48939
- [19] “Propellant, Hydrogen Peroxide,” U.S. Department of Defense, Performance Spec. MIL-PRF-16005F, 2003.
- [20] Gordon, S., and McBride, B. J., “Computer Program for Calculation of Complex Chemical Equilibrium Compositions and Applications,” NASA Ref. Publ. 1311, 1994.
- [21] Sutton, G. P., *Rocket Propulsion Element*, 7th ed., Wiley Interscience, New York, 2001.

D. Talley
Associate Editor